NUMERICAL AND EXPERIMENTAL INVESTIGATION OF FLOW FIELD INSIDE ARTERIES AND VEINS

Prof.Dr. Najdat Nashat Abdulla
Asst.Prof. Hussain Yousif Mahmood
Graduate Student Sadiq Elias Abdullah
Department of Mechanical Engineering

University of Baghdad

ABSTRACT

Numerical and experimental investigation of blood flow through stenotic and tapered arteries under pulsation condition are studied. Blood is considered as non-Newtonian fluid. Artery is considered as a rigid wall tapered vessel with different tapering angles (0.5^o, 1^o,1.5^o), as well as, straight vessel for comparison. The governing equations have been written in stream- vorticity method and are transformed into generalized coordinate system. The time marching has been employed to solve the resulting partial differential equations. The experimental work carried out to examine pressure in vessel and pressure drop across the stenosis under pulsation condition. Differential pressure transducer coupled to the data acquision card type PCI-911DG, which is built in computer was used to record pressure data.

The results showed that, as a tapering angle increases (0.5^o, 1^o, 1.5^o) both wall shear stress and pressure drop increasing, also as stenosis increases (50%, 60%, 75%) both wall shear stress and pressure drop increasing. These behaviors are found in literature, pressure drop is used to compare experimental data and numerical results, which indicates agreement. As the distance into taper section increased both wall shear stress and pressure drop are increased, as well as, both wall shear stresses and pressure drop increased with inlet flow rate increased, while decreased with inlet diameter increase.

الخلاصة

تم أجراء دراسة عددية و تجريبية لجريان الدم خلال شريان متضايق و مستدق تحت شرط الجريان النبضي. أعتبر الدم غير نيوتوني وتم أخذ شريان ذو جدار متصلب ومستدق بزوايا مختلفة **(1.5, 1, 0.5)** درجه وتمت مقارنته مع شريان مستقيم. كتبت المعادلات الحاكمة بطريقه داله الانسياب– الدواميه وحولت هذه المعادلات إلى نظام إلاحداثيات العمومية 0 كما استخدم طريقه الزحف الزمني لحل المعادلات التفاضلية الجزئية الناتجة. جرى العمل التجريبي لاختبار الضغوط عبر أنبوبه ذات تضبق

تحت شروط الجريان النبضي و الذي تم بواسطة مقياس الضغط التفاضلي (**Transducer**) مرتبط بمعالج بيانات نـــوع **PCI-911DG** مثبت في حاسوب لتسجيل الضغوط.

أظهرت النتائج أنه عند زيادة زاوية الأستدقاق (**0.5 , 1 , 1.5**) درجة تزداد كلا من أجهاد القص على الجدار و هبوط الضغط و كذالك فأنه بزيادة نسبة التضيق (**50% , 60% , 75%**) , فأن أجهاد القص على الجدار يزداد وهذا السلوك وجـــد في البحوث السابقة0 كما تبين أنه بزيادة نسب التضيق يزداد هبوط الضغط وهذا يبين التطابق بين النتائج النظرية و التجريبيـــة 0 وكذالك تزداد كلا من أجهاد القص على الجدار و هبوط الضغط كلما زادت المسافة باتجاه نهاية الاستدقاق, وأظهرت النتائج زيادة كلا من أجهاد القص على الجدار و هبوط الضغط بزيادة التدفق الداخل ,بينما يقلان بزيادة قطر أنبوب الدخول0

INTRODUCTION

Considerable attention was paid to study related circulatory flow in blood vessels toward the beginning of the last century. A large number of theoretical and experimental Investigations relevant to this biomechanical aspect have been carried out in recent years. Hardly need mention that, about three quarter of all death occurring these days are mainly caused by circulatory diseases associated with disturbed flow condition in the blood vessels which lead to the malfunction of the cardiovascular **(Chen 2003).** The presence of stenosis increases flow resistance in arteries which forces the body to raise the blood pressure to maintain the necessary blood supply. Both the high blood pressure and narrowing blood vessel cause high flow velocity, high shear stress and low or negative pressure at the throat of the stenosis .In addition to low shear stress, flow separation and wall compression or even collapse at the distal side of stenosis .This may related to the thrombus formation, atherosclerosis growth and plaque cap rupture which lead directly to stroke and heart attack.

Several studies of fluid dynamics through stenosis have been carried out to evaluate the flow pattern and the shear stress at walls at steady and pulsate flow conditions .Some attempts to study experimentally**,(Walburn and Stein 1981**) measured velocity with Laser Doppler anemometer in plexiglass tube with tapered of 0.5^o, 1.5^o and 2.5^o, measured from centerline to the wall during steady flow. These angles were comparable to the angles of taper observed in abdominal aorta of normal subject 1.5^o. $\pm$ 0.2^o "range 0^o to 3^o" as reported. They calculated transition Reynolds number which based on diameter of tube at point of measurement. The results show increasing of transition Reynolds number with increasing angle of tapering, also with increasing distance into tapered section for constant angle of taper. These observations suggested that, tapering of abdominal aorta tends to promote laminar flow.**(Ojha, et al 1989)**, used a photochromic tracer method to record pulsatile flow velocity profiles simultaneously at three axial locations along a flow channel. Thereby enabling the time and spatial distribution of the wall shear stress to be studied, as well as visualizing of the flow. In addition, they studied the transition to turbulence triggered by the moderate stenosis. Asymmetric and axisymmetric stenosis models were used. Shape of stenosis were based on clinic observations , percent of area reduction were 45%,65% and 75% for axisymmetric ,while 38% "of total area cross section " for asymmetric stenosis .The work was done for Reynolds number in the ranges of 380-575 and Womersley number of 7.5.

Other numerical studies deal blood as non Newtonian fluid, **(Pontrelli 1999)** investigated steady axisymmetric flow in a constricted rigid tube. A shear- thinning fluid which modeling the deformation dependent viscosity of blood .The governing equation was written in vorticity–stream function and solved numerically by finite difference method. The constriction was described by exponential function. The results demonstrate that, the non-Newtonian character of the blood in some typical regimes modify the flow pattern even beyond the constricted region, reduce the pressure drop and shear stress at the wall across the stenosis**.(Kimmel and Dinnar 1983)** , modeled blood flow through a segment of large arteries between bifurcations as pulsate flow of Newtonian fluid in tapered converging tubes of small angle of converging up to 2 degree .In this study, flow rate considered as a

forcing function rather than uniform pressure gradient .Integral method was used in solution of Navier –Stokes equations. The result showed that, change in flow condition due to tapering of blood vessel are significant even for small tapering angle and cannot be ignored. Also as tapering angle increases, peak shear stress at wall also increases, but still below the critical range which lead to damage of endothelial. **(Porenta et al 1985)**, used a finite element method to model pulsating flow in arteries segment including taper, branch, and obstructions. In branch model ,they assumed that the pressure different across location where branch diverter from the main stream was small and can be neglected, while in obstructions model ,they calculate pressure difference across stenosis .The results indicate that, the pressure wave were traveling along artery shows an amplification in distal direction ,and they conclude that each nonlinear term contributes to the effect noticed in the nonlinear case .While the influence of the convective acceleration term in momentum equation was stronger ,also the combined effect of both nonlinearities was larger than the added effect of each individual term .The effect of stenosis on pressure shows that the distal pressure for 50% stenosis only slightly reduced, and distal flows were slightly damped ,while for high stenosis (75% and 90 %) had large effect. Wall shear stress is an important factor in the study of blood flow ,and an accurate predication of the distribution of wall shear stress are particularly useful for understanding the effect of blood on endothelial cells. **(Guo-Tao et al. 2004)** investigated distribution of wall shear stress by simulation of pulsating blood flow through stenotic tapered artery .The incompressible Navire-stokes equations were solved numerically by a finite difference method .The results indicated that, the height of stenosis was more important factor influencing blood flow than wall tapering. Tapering found to have no effect on flow pattern, but only change the value. On the other hand, it becomes bigger value than without tapering; also the peak value of shear stress of tapered artery was bigger than that without taper. In parallel work, **(Hun Jung et al, 2004)** used a finite volume method to solve three dimensional, fully developed flows and blood taken as a non Newtonian fluid which obeys to Carreau-Yasuda. They compared the results with **(Ojha et al 1989)** for case of 45% stenosis trapezoidal profile, and a good agreement was shown .For cosine profile stenosis, a numerical computational was conducted for 50 %and 75% stenosis, and the result showed that, the severity of the stenosis had significant effect on the general flow features such as separation Reynolds number and size of the separation region, while the shape of stenosis had less effect. Also, it showed that, the peak values of wall shear were exerted at the stenosis and negative shear stress were observed in the region where a vortex exists. Summary of the past studies indicated that, the flow of non-Newtonian fluid though constricted taper artery under pulsation condition was not considered .As a conclusion, **(Guo-Tao et al.2004)**, considered Newtonian fluid through constricted taper pipe, but only for small angle 0.5^{o}, while the present study extended to involve 1^{o}, and 1.5^{o}. Also noted that, **(Hun-jug et al. 2004)**, considered flow of non-Newtonian fluid through constricted tube under pulsating condition , but they ignored effect of tapering and restricted the study to small percent of stenosis(25%,33%,50%),which its effect was small on pressure drop across stenosis **(Porenta et al. 1985)**.

The present work will consider the flow of non-Newtonian fluid through constricted artery under pulsation condition for tapering angles up to 1.5^{o} and percent of stenosis up to 75%.Numerical and experimentally investigations of blood flow through constricted taper artery are carried at pulsation condition for vessels with 50%, 60% and 75% stenosis. Blood considered as a non-Newtonian fluid obeying the shear thinning model

MATHEMATICAL MODEL AND NUMERICAL CALCULATION

The governing equations of blood flow through stenosis artery at pulsation condition are formulated and stated in polar coordinate. The working fluid is considered as a Non-Newtonian fluid and incompressible.

A schematic of the stenosis tube geometry considered in this study is shown in **Fig. (1),** which consists of two main parts, tube and the stenosis, stenosis geometry is shown in **Fig.(2)**

Let us now consider a cylindrical coordinate system (x,r,θ) having the x-axis coincident with the pipe axis .since we seek an axisymmetric 2D solution ,all variable are assumed independent of θ and the azimuthal component of v vanishes ,equation of motion can be written as follows:

$$\rho(\frac{\partial u}{\partial t}+u\frac{\partial u}{\partial x}+v\frac{\partial u}{\partial r})=-\frac{\partial p}{\partial x}+2\frac{\partial \mu}{\partial x}\frac{\partial u}{\partial x}+\frac{\partial \mu}{\partial r}(\frac{\partial v}{\partial x}+\frac{\partial u}{\partial r})+\mu(\frac{\partial^2 u}{\partial x^2}+\frac{\partial^2 u}{\partial r^2}+\frac{1}{r}\frac{\partial u}{\partial r}) \quad (1)$$

$$\rho(\frac{\partial v}{\partial t}+u\frac{\partial v}{\partial x}+v\frac{\partial v}{\partial r})=-\frac{\partial p}{\partial r}+\mu(\frac{\partial^2 v}{\partial x^2}+\frac{\partial^2 v}{\partial r^2}+\frac{1}{r}\frac{\partial v}{\partial r}-\frac{v}{r^2})+\frac{\partial \mu}{\partial x}(\frac{\partial v}{\partial x}+\frac{\partial u}{\partial r})+2\frac{\partial \mu}{\partial r}\frac{\partial v}{\partial r} \quad (2)$$

Where (u ,v) are the components of V in the r and x directions respectively.

Complex rheological behavior of blood is approximated using a shear thinning model, where the apparent viscosity is expressed as a function of the shear rate **(Pontrelli 1999)** and **(Hun Jung et al 2004)**.

$$\mu(\dot{\gamma})=\eta_\infty+(\eta_o-\eta_\infty)(\frac{1+\log e(1+\wedge\dot{\gamma})}{1+\wedge\dot{\gamma}}) \quad (3)$$

Where

η_o and η_∞ are asymptotic viscosities as $\dot{\gamma}\to 0$ and ∞ respectively

$\wedge$ is a materiel constant with dimension of time representing the degree of shear thinning .

$\dot{\gamma}$ shear rate which represents a scalar measure of the rate of deformation is given by **(Pontrelli 1999)** and **(Hun Jung et al 2004)**

$$\dot{\gamma}^2=\frac{1}{2}\sum_i\sum_j e_{ij}e_{ji} \quad (4)$$

To non-dimensionalized the governing equations, a set of variables are introduced **(Pontrelli 1999)**

$$x=\frac{x}{R},\ r=\frac{r}{R},\ t=t*f,\ u=\frac{u}{V},\ v=\frac{v}{V},\ p=\frac{p}{0.5\rho V^2},\ \Lambda=\frac{\Lambda V}{R},\ \delta=\frac{\eta_0}{\eta_\infty}$$

Where: R= vessel inlet radius and V =average velocity at inlet

eq.(1) can be written in following form

$$\frac{\lambda^2}{\mathrm{Re}}(\frac{\partial u}{\partial t}+u\frac{\partial u}{\partial x}+v\frac{\partial u}{\partial r})=-\frac{\partial p}{\partial x}+\frac{1}{\mathrm{Re}}[2\frac{\partial \dot{X}}{\partial x}\frac{\partial u}{\partial x}+\frac{\partial \dot{X}}{\partial r}(\frac{\partial v}{\partial x}+\frac{\partial u}{\partial r})+\dot{X}(\frac{\partial^2 u}{\partial x^2}+\frac{\partial^2 u}{\partial r^2}+\frac{1}{r}\frac{\partial u}{\partial r})] \quad (5)$$

and **eq.(2)** can be written in following form

$$\frac{\lambda^2}{\mathrm{Re}}(\frac{\partial v}{\partial t}+u\frac{\partial v}{\partial x}+v\frac{\partial v}{\partial r})=-\frac{\partial p}{\partial r}+\frac{1}{\mathrm{Re}}[\dot{X}(\frac{\partial^2 v}{\partial x^2}+\frac{\partial^2 v}{\partial r^2}+\frac{1}{r}\frac{\partial v}{\partial r}-\frac{v}{r^2})+\frac{\partial \dot{X}}{\partial x}(\frac{\partial v}{\partial x}+\frac{\partial u}{\partial r})+2\frac{\partial \dot{X}}{\partial r}\frac{\partial v}{\partial r}] \quad (6)$$

Where: $\lambda=R\sqrt{\frac{f}{\upsilon}}$ Womersley number , $\mathrm{Re}=\frac{\rho uR}{\mu}$ Reynolds number; f= Frequency of pulsation

$\dot{X}$ = Non dimensional viscosity which is given below

$$\dot{X}(\dot{\gamma}) = 1 + (\delta - 1)[\frac{1 + \log e(1 + \wedge \dot{\gamma})}{1 + \wedge \dot{\gamma}}] \quad (7)$$

Stream – vorticity approach

By cross differentiating and by subtracting the counterparts of **eqs(5**) and **(6)**, we obtain the vorticity –stream function formulation :

$$\frac{\lambda^2}{\mathrm{Re}}\frac{\partial \omega}{\partial t} - \frac{1}{r}\frac{\partial \psi}{\partial x}\cdot\frac{\partial \omega}{\partial r} + \frac{\omega}{r^2}\frac{\partial \psi}{\partial x} + \frac{1}{r}\frac{\partial \psi}{\partial r}\cdot\frac{\partial \omega}{\partial x} = \frac{1}{\mathrm{Re}}[\frac{\partial \dot{X}}{\partial x} * 2\frac{\partial \omega}{\partial x} + \dot{X}(\frac{\partial^2 \omega}{\partial x^2} + \frac{\partial^2 \omega}{\partial r^2} + \frac{1}{r}\frac{\partial \omega}{\partial r} - \frac{\omega}{r^2})$$
$$+ (\frac{\partial^2 \dot{X}}{\partial x^2} - \frac{\partial^2 \dot{X}}{\partial r^2})(\frac{1}{r}\frac{\partial^2 \psi}{\partial r^2} - \frac{1}{r}\frac{\partial^2 \psi}{\partial x^2} - \frac{1}{r^2}\frac{\partial \psi}{\partial r}) + \frac{\partial \dot{X}}{\partial r}(2\frac{\partial \omega}{\partial r} + \frac{\omega}{r}) + 2\frac{\partial^2 \dot{X}}{\partial x \partial r}(\frac{1}{r^2}\frac{\partial \psi}{\partial x} - \frac{2}{r}\frac{\partial^2 \psi}{\partial x \partial r})] \quad (8)$$

and shear rate can be written as follows

$$\dot{\gamma}^2 = \frac{1}{r^2}(\frac{\partial^2 \psi}{\partial r^2} - \frac{\partial^2 \psi}{\partial x^2} - \frac{1}{r}\frac{\partial \psi}{\partial r})^2 + \frac{4}{r^2}[(\frac{\partial^2 \psi}{\partial x \partial r})^2 - \frac{1}{r}(\frac{\partial \psi}{\partial x})(\frac{\partial^2 \psi}{\partial x \partial r}) + \frac{1}{2r^2}(\frac{\partial \psi}{\partial x})^2] \quad (9)$$

Vorticity and stream function are related by poisson equation:

$$\frac{\partial^2 \psi}{\partial x^2} + \frac{\partial^2 \psi}{\partial r^2} - \frac{1}{r}\frac{\partial \psi}{\partial r} = -\omega r \quad (10)$$

Stream – vorticity approach obtained by eliminating the pressure terms from the momentum equations. Since its important to know pressure drop to used to compare numerical results and experimental data, the pressure drop along x- axis derived from momentum equation for steady incompressible, and non – Newtonian fluid **eq.(5**), **(Nallasamy 1986)**.pressure drop calculated from following equation:

$$\frac{dp}{dx} = \frac{1}{\mathrm{Re}}[\dot{X}(-\frac{\partial \omega}{\partial r} - \frac{\omega}{r}) + \frac{\partial \dot{X}}{\partial r}(\frac{1}{r}\frac{\partial^2 \psi}{\partial r^2} - \frac{1}{r}\frac{\partial^2 \psi}{\partial x^2} - \frac{1}{r^2}\frac{\partial \psi}{\partial r})] \quad (11)$$

Also, shear stress at wall is important factor which has direct effects on internal layer of vessel, where a high value of shear stress leads to damage in vessel wall, shear stress at wall calculated from equation:

$$\therefore \tau_{wall} = \frac{\omega_{wall}}{\mathrm{Re}} \quad (12)$$

Initial and boundary conditions

To solve vorticity transport equation **eq(8)** and Poisson equation **eq.(10),** it required that, the appropriate expressions for stream function ψ and vorticity ω be specified at the boundary **(Anderson et al 1984)**. The specification of these boundary conditions is extremely important since it directly affects the stability and accuracy of the solution. It is important and care must be taken to ensure that the physics of the problem is correctly modeled, on how to treat these geometries or models.

Hence the boundary conditions are summarized as follows:-

1- At tube center line:

Vorticity and stream function sets equal zero, $\psi = 0$, $\omega = 0$

2- At tube wall:

Since no-slip condition at wall, velocity component equal zero, stream function set

$$\psi_{wall} = q/2 \quad (13)$$

Where q is flow rate for real situation **(Taylor et al 1998)**, the flow changes as shown in **Fig.(3).** While vorticity at wall derived form Poisson **eq. (10)**, with $\frac{\partial \psi}{\partial r} = 0$ (no slip condition), for that **eq.(10)** can be written as **(Agrawal and Sengupta 1989)** and **(Cheng et al 1974)**.

$$\omega_{wall} = \frac{1}{R}\left(\frac{\partial^2 \psi}{\partial x^2} + \frac{\partial^2 \psi}{\partial r^2}\right) \quad (14)$$

3- At tube inlet:

Since the flow at inlet uniform, the vorticity value will set equal zero, while stream function at inlet varied form zero at center line to value of **eq. (13)**.

4- At tube exit:

At exit, the variation in vorticity and stream function is negligible

$$\frac{\partial \psi}{\partial x} = \frac{\partial \omega}{\partial x} = 0 \quad (15)$$

5-Initial condition:

Assume no flow, then stream function and vorticity set equal to zero.

Since the stenosis artery is a complex domain, therefore, the governing equations are transformed from polar coordinate to generalized coordinate.

TRANSFORMATIONS OF GOVERNING EQUATIONS

Transformation stream- vorticity equation:-

$$-\omega r J^2 = \psi_{\zeta\zeta}\alpha + \psi_{\eta\eta}\gamma - \psi_{\zeta}\frac{x_{\eta} J}{r} - \psi_{\eta}\frac{x_{\zeta} J}{r} - 2\beta\psi_{\zeta\eta} \quad (16)$$

$$\alpha = x_{\eta}^2 + r_{\eta}^2 \; : \; \gamma = x_{\zeta}^2 + r_{\zeta}^2 \; : \; \beta = x_{\zeta} x_{\eta} + r_{\zeta} r_{\eta} \quad (17)$$

Transformation vorticity transport equation:-

$$\frac{\lambda^2}{\mathrm{Re}}\frac{\partial W}{\partial t} + \frac{1}{r}(\psi_{\zeta} x_{\eta} - \psi_{\eta} x_{\zeta})(\omega_{\zeta} r_{\eta} - \omega_{\eta} r_{\zeta}) \, 1/J - \frac{1}{r}[\psi_{\zeta} r_{\eta} - \psi_{\eta} r_{\zeta}]$$

$$[\omega_{\eta} x_{\zeta} - \omega_{\zeta} x_{\eta}] * 1/J + \frac{\omega}{r}[\psi_{\zeta} r_{\eta} - \psi_{\eta} r_{\zeta}) \frac{1}{J} =$$

$$\frac{1}{\mathrm{Re}}[(\dot{X}_{\zeta} r_{\eta} - \dot{X}_{\eta} r_{\zeta})(\omega_{\zeta} r_{\eta} - \omega_{\eta} r_{\zeta}).\frac{2}{J} + \dot{X}(\omega_{\eta}\frac{x_{\zeta}.J}{r} - \omega_{\zeta}\frac{x_{\eta}.J}{r} + \alpha\omega_{\zeta\zeta} +$$

$$\gamma\omega_{\eta\eta} - 2\beta\omega_{\zeta\eta} - \frac{\omega.J^2}{r^2}) * \frac{1}{J^2} + (\dot{X}_{\zeta\zeta}\alpha_x + \dot{X}_{\eta\eta}\gamma_x + 2\dot{X}_{\zeta\eta}\beta_x)/J^2 * (\frac{1}{r}(\psi_{\zeta}\frac{r_{\eta}.J}{r} -$$

$$\psi_{\eta}\frac{x_{\zeta} J}{r} + \alpha_r\psi_{\zeta\zeta} + \gamma_r\psi_{\eta\eta} - 2\beta_r\psi_{\zeta\eta})\frac{1}{J^2} + (\dot{X}_{\eta}\frac{x_{\zeta}}{J} - \dot{X}_{\zeta}\frac{x_{\eta}}{J})(2(\omega_{\eta}\frac{x_{\zeta}}{J} - \omega_{\zeta}\frac{x_{\eta}}{J}) +$$

$$\frac{\omega}{r}) + 2/J^2[\dot{X}_{\zeta\eta}(r_{\eta}x_{\zeta} + r_{\zeta}x_{\eta}) - \dot{X}_{\zeta} r_{\zeta}x_{\zeta} - \dot{X}_{\eta\eta} x_{\eta}r_{\eta}] * [\frac{1}{r^2}(\psi_{\zeta}\frac{r_{\eta}}{J} - \psi_{\eta}r_{\zeta}/J) -$$

$$\frac{2}{r}(\psi_{\zeta\eta}(r_\eta x_\zeta + r_\zeta r_\eta) - \psi_{\zeta\zeta} x_\zeta r_\zeta - \psi_{\eta\eta} r_\eta x_\eta) * {}^{1}\!/_{J} \ ] \tag{18}$$

Transformation of pressure drop equation:-

$$\frac{dp}{dx} = -\dot{X}\left(\left(\omega_\eta x_\zeta - \omega_\eta x_\eta\right)/J + \frac{\omega}{r}\right)\left(\dot{X}_\eta x_\zeta - \dot{X}_\zeta x_\eta\right)1/J *$$

$$\frac{1}{r}[\psi_\zeta \frac{x_\eta . J}{r} - \psi_\eta \frac{x_\zeta . J}{r} + \alpha_r \psi_{\zeta\zeta} + \gamma_r \psi_{\eta\eta} - 2\beta_r \psi_{\zeta\eta}) * \frac{1}{J^2} \tag{19}$$

Transformation of shear rate equation:-

$$\dot{\gamma}^2 = \frac{1}{r^2}\left[(\alpha_r \psi_{\zeta\zeta} + \gamma_r \psi_{\eta\eta} - 2\beta_r \psi_{\zeta\eta} + \frac{\psi_\zeta x_\eta J}{r} - \frac{\psi_\eta x_\zeta J}{r}) {}^{1}\!/_{J^2} \ \right]^2$$

$$+\frac{4}{r^2}\left[((\psi_{\zeta\eta}(r_\eta x_\zeta + r_\zeta x_\eta) - \psi_{\zeta\zeta} x_\zeta r_\zeta - \psi_{\eta\eta} x_\eta r_\eta) {}^{1}\!/_{J^2})^2 + \frac{1}{2r^2 J^2}(\psi_\zeta r_\eta - \psi_\eta r_\zeta)^2\right.$$

$$\left. + \frac{J}{r}(\psi_\zeta r_\eta - \psi_\eta r_\zeta) * [(\psi_{\zeta\eta}(r_\eta x_\zeta + r_\zeta x_\eta) - \psi_{\zeta\zeta} x_\zeta r_\zeta - \psi_{\eta\eta} x_\eta r_\eta) {}^{1}\!/_{J^2}]\right. \tag{20}$$

Transformation of boundary equation:-

$$\omega_{wall} = \frac{\gamma}{r.J^2}(\psi_{\eta\eta}) \tag{21}$$

Grid Generation

The most common partial differential equation uses for grid generation in two dimensional is a Poisson equation in the form **(Fletcher 1987)** and **(Anderson 1984)**.

$$\alpha x_{\zeta\zeta} - 2\beta x_{\zeta\eta} + \gamma x_{\eta\eta} = -[x_\zeta P(\zeta,\eta) + x_\eta Q(\zeta,\eta)]/J^2 \tag{22}$$

$$\alpha r_{\zeta\zeta} - 2\beta r_{\zeta\eta} + \gamma r_{\eta\eta} = -[r_\zeta P(\zeta,\eta) + r_\eta Q(\zeta,\eta)]/J^2 \tag{23}$$

Where

$\alpha = x_\eta^2 + r_\eta^2$, $\gamma = x_\zeta^2 + r_\zeta^2$, $\beta = x_\zeta x_\eta + r_\zeta r_\eta$ and $J = x_\zeta r_\eta - x_\eta r_\zeta$

all grids used in this investigation are generated with $P(\zeta,\eta)=Q(\zeta,\eta)=0$.(**Bramley and Sloan 1987)** and **(Ali 2002)**.The non linear difference equations are solved iteratively using a point SOR method and, at each cycle of iteration, the coefficients α, β and γ are evaluated using previous approximations. **Fig.(4.a)** and **Fig.(4.b)** show the physical and computational domains which are used in the present study.

Time Marching

The basic principle of time marching is to start from an initial guess of the flow pattern, then the method solves the unsteady continuity, momentum equations for the evolution of the flow in time until equilibrium is established. Basically, the flow region is divided in to a grid network so that different terms in the governing equations are defined at each grid point. The flow field is then solved from the governing equations in finite difference form subjected to the imposed boundary conditions. With the flow equations applied to each grid point in turn, the solution becomes closer to the unsteady state solution for each time step **(Iatridis 1987)**.

Experimental Work

The rig was designed to simulate the blood flow through constricted artery, which must satisfy number of requirements: pulsation flow, non-Newtonian fluid, taper vessel, stenosis vessel, developing flow and Laminar flow as shown in **Fig.(5).**

Dosing pump type **ALLDOS** Model EN600034 with flow rate 115 L/h, 3 bars, power 0.09Kw, 0.88-0.9 Ampere and 1270 RPM is used, which its operation is based on using diaphragm movement by rode connected eccentric disc, to generate pulsating flow. In order to measure a pressure drop in the test section under pulsation condition, the differential pressure transducer type **FOXPRO** with range of 20 mbar is used. Its operation is based on diaphragm movement and converting the pressure drop to electrical signal**.** Switch flow meter with range of 130L / h which gives indication for the number of pulses in sec and frequency .Flow meter is connected with interface card and accessed to computer. The amount of flow rate was measured by collecting working fluid in container and time was accounted by stop watch. To simulate the fluid dynamic behavior of blood, a solution of 2:3 glycerin-water with density of 1.120 g/cm^3 and viscosity (3.5 - 4) C.P. was used **(Rose et al 1998), (Cebral et al 2002)**.Density and viscosity were measured every day before starting to record data .To simulate the artery Acrylic tube with inlet diameter 16,18 and 20 mm **(Cox et al 1979)** and **(Wellborn and Stein 1981)**,with taper angle for each size (0.5, 1 and 1.5 degree) were used **(Walburn and Stein 1981),(Kimmel and Dinnar 1983)**.The length of test section was 175 mm **(Walburn and Stein 1981)** and 10 mm threaded added in entrance to use in connection with Acrylic block. The taper of inside diameter of tube match taper angle of out side diameter of stenosis to fix the stenosis in first third length of tube. Small tap was used upstream of joins block to prevent bubbles to inter test section.

Stenosis model is made from Acrylic with trapezoidal shape **(Ojha et al 1989)** and **(Varghese and Frankel 2003)** as shown in **Fig.(2).**

Five taps with sizes according to ISO standard 5167 **(Miller 1983)** were drilled in test section and locations of taps are shown in **Fig.(6)** . A copper tube with 4mm out diameter was fixed on taps (1, 2, 4, and 5) by epoxy, as shown in section (A), while bolt (M4) was used for tap (3), which required a special connection, as shown in section (B).

Data acquisition card type PCI-9111 is used, this data acquisition card is based on the 32-bit PCI bus architecture. High performance design and the state-of-the-art technology make this card ideal for data logging and signal analysis application in areas like medicine and process control, **(Aimen 2005)**. In order to read the signal from the Pressure Transducer and Swatch flow meter sensor a program is required to record signal. Before writing this program it is necessary to ensure that the MATLAB defines the DAC in its tools.

Results and Discussion

To study the influence of stenosis and taper on blood "Non – Newtonian fluid" flow through artery, the computations were conducted for various stenosis severity (50%, 60% and 75%) and different values of tapering vessel angles (0, 0.5^o, 1^o, and 1.5^o). To perform a careful parameter analysis, the instantaneous streamlines are calculated and shown during cycle of pulsation flow at intervals of 0.1 sec. The non – dimensional Womersley and Reynolds numbers are considered as 7.1 and 50 respectively .The study was carried out under constant flow rate.

Numerical results

As a first step in the analysis, a check for validation program is performed through the comparison of numerical results with results of **(Pontrelli 1999)**, for steady flow, Newtonian and non-Newtonian fluid at a Reynolds number of 10. The stenosis profile used in this comparison is described as exponential function. The stream at wall "maximum stream function" is 50 **(Pontrelli 1999)**. Comparison shown in the **Fig.(7)** and **Fig.(8)** which indicated that ,the present result has higher values than results in **(Pontrelli 1999)**, for both cases Newtonian fluid and Non – Newtonian fluid .The difference in results is due to method of calculation, the used equation in calculation of wall shear stress and input parameter of **(Pontrelli 1999)**.

The numerical study is carried out under pulsation condition, Re. No. = 50 and Womersley No. =7.1.Blood is considered as a non- Newtonian fluid with parameter Λ =50 which represents the degree of shear – thinning and for ratio of asymptotic viscosities at zero and infinity equal to δ = 40 **(Pontrelli 1999)**. The number of grid points along the axis in (ζ, η) is (176, 16), the time step has been selected as small $\Delta T=10^{-7}$ compared to $\Delta T=10^{-6}$ for steady case [Pontrelli 1999] in order to guarantee the convective and diffusive stability condition in all cases [Fletcher 1987,1].Different angles of vessel tapering ($0,0.5^o,1^o,1.5^o$) with different degree of stenosis (0,50%,60%,75%) are considered. Streamline, wall shear stress and pressure drop results are plotted and studied.

Streamline distributions inside blood vessel at each time step are plotted for different stenosis present and different vessel tapers. The results indicate that, the stream line changes as inlet flow rate change as shown in **Fig.(9)** , the separation region is noted clearly at time step 0.4 sec and grows as time advanced. Also it can be noted that, the separation region upstream of stenosis showed to be started at time step 0.8 sec .The WSS distribution for tapered vessel 1.5^o, with 75% stenosis is shown in **Fig.(10).** Due to taper angle, the WSS increases as distance increased into tapered section, the peak value of WSS is shown at stenosis part. While the WSS values at time step 0.4 sec, 0.5 sec, 0.7 sec and 0.8 sec are not increased due to low inlet flow rate at these time steps. At time step 0.7 sec and 0.8 sec negative values of WSS are indicated. The WSS distribution indicated same behavior as seen when stenosis 60% but a lower reduction is observed with negative value of WSS at time step 0.8 sec, also this effect become lower at 50% stenosis. Comparison WSS of distributions at some instantaneous times reveals that, the highest of stenosis has a significant influence on the WSS at the throat, the downstream of throat, and the length of separation region. Since high WSS is not only damage the vessel wall and causes intimal thickening, but also it actives platelets which causes' aggregation, and finally results in the formation of a thrombus, the wall shear stress at throat deserves to be noticed **(Guo-Tao et al 2004)**.

Pressure drops along the axial length of vessel are plotted, which indicated that, the pressure drops at stenosis part and this drop in pressure reduces at distal stenosis. Also, pressure drop changes as the inlet flow rate changes at each time step. Further, the drops change according to the stenosis percent changes. **Fig.(11)** shows pressure drop along the axial length and the pressure drop changes as inlet flow rate changes. A high reduction in pressure is observed at time step 0.2 sec and 0.3 sec for high flow rate. Pressure at distal stenosis was higher than pressure at proximal stenosis due to the back flow at distal stenosis.

Experimental Results

Experimental work was conducted at Re.No.= 580, Womersley No.= 6.3, and frequency= 2.1Hz. The density of the working fluid was taken as 1.120 g/cm^3 and the viscosity in rang of (0.035-0.04) Posie. Test was carried out at an average flow rate of 51 ml/sec and the data recorded at rate of 1280 samples for duration of 51sec.As the stenosis is increased the pressure difference increased. As the stenosis increase the cross sectional area decreases and flow accelerates, consequently, the pressure energy is converted to the kinetic energy. The reduction in pressure can be calculated from Bernoulli's equation and it can be written as follows **(Walburn and Stein 1981)**:

$$\Delta p = 0.5\rho V^2((\frac{D}{d_m})^4 - 1) \quad (24)$$

Where d_m is diameter of center stenosis: D is diameter upstream stenosis
It is clear that, diameter of stenosis had a direct effect on value of pressure drop value, and power index "four" explain the difference in pressure drop for different percent stenosis (50%, 60% and 75%) as shown in **Fig.(12).**This results are in agreement with the results of **(Porenta et al 1985)**, **(Bapat 2005)**, and consistence with the general observation of the effect stenosis of less than 50% have little effect on pressure and flow .This is one of the reason why stenosis are difficult to diagnose at an early stage. The pressure difference in all measurements are non dimensionalzed with $(\frac{1}{2}\rho V^2)$ for all the cases. In taper section, the flow is accelerated and energy is converted from pressure energy to kinetic energy. This reduction in pressure energy can be calculated by substituting the continuity equation into the Bernoulli equation, with some manipulation, yields **(Walburn and Stein 1981)**.

$$\Delta p = 0.5\rho V^2[(\frac{D}{D - 2l\tan\theta})^4 - 1] \quad (25)$$

eq.(25) indicate that, as tapering angle increases the pressure drop increase as shown in **Fig.(13),** also the pressure drop increases as distance of taper section increases.

Comparisons

To check the validity of the numerical technique, several comparisons of numerical results for different cases are performed at time step 0.2 sec, where the discrepancy is clear and this is due to the maximum flow rate. Experimental results for pressure drop are compared with numerical results and with available literature for same cases.

The effect of different percent stenosis on the WSS for 1.5^o taper vessels are shown in **Fig.(14),** which indicates that, as stenosis degree increases WSS increases and the same trend is by **(Hun Jung et al 2004)**.

Pressure drop plots are used for comparison of numerical results with experimental data for the present study to investigate the effects of stenosis percent for different taper vessels .**Fig.(15)** indicates that, the pressure drop increases as degree of stenosis increases in straight vessel and a high pressure difference is found at 75% stenosis compared with 50% and 60% stenosis .This behavior was in agreement with **(Bapat 2005)** as shown in **Fig.(16).**It indicates that, present experimental data has a higher value, this due to constant viscosity and shape of stenosis used by **(Bapat 2005)**, also it is coincident with the conclusion of the survey investigated by **(Young 1979)**.

On the other hand, the effects of tapering angle are investigated with and without stenosis. For case of without stenosis, comparison of experimental data with **(Walburn and Stein 1981)** is preformed as shown in **Fig.(17)** .It is clear that, present data have higher values than **(Walburn and Stein 1981)** data ,this is due to the viscosity (0.0103 Poise) compared with a mixture fluid with viscosity in range (0.035 to 0.040 Poise) in present study. Also as tapering angle increases WSS increases, and this is clearer at the end of the vessel. This is in agreement with **(Kimmel and Dinnar 1983)** as shown in **Fig.(18).**It shows that , the values of WSS in the present study are higher than

(Kimmel and Dinnar 1983) values, because they are assumed Newtonian fluid, different input flow rate and one dimension flow .

In order to compare the numerical results with experimental data in the present study, calculations are preformed with sine wave profile inlet flow rate to confirm the experimental work with Re.No.= 580 and Womersley No.= 6.3 as shown in **Fig.(19).** This indicate that, the numerical results have same behaviors as experimental results, but with higher values

Conclusions

Computational and experimental simulations for blood flow through stenosis artery under pulsation condition were carried out in this study. A shear thinning model was used to express Blood, which is considered as non-Newtonian fluid. Attention was focused on the effect of stenosis on pressure drop and wall shear stress. The following are the main conclusions drawn from the present investigation work ,Both pressure drop and wall shear stress were increased as taper angle of vessel increase (0.5^o, 1^o, 1.5^o), due to increase in kinetic energy, also increased as stenosis increase (50%, 60% and 75%), and a large effect seen for 75% stenosis.

Wall shear stress had negative values where vortex exists, vortex region may be the origin of red cell damage and thrombus formation and the stenosis will progress further, and the high stress is exerted near the stenosis throat of blood vessel due to fast flow and will generate serious physical damages. Tapering of the artery did not change flow patterns, but only changed values, amplified the values of wall shear stress and pressure drop. As the distance into taper section increased both pressure drop and wall shear stress were increased. Both pressure drop and wall shear stress were increased as the distance into taper section increased. For the stenosis percent less than 50% a little effect on pressure and flow was seen. This is a reason for why the stenosis percent are difficult to diagnosis at an early stage.

As a related to the present work, following suggestions can be put forward. Vessel wall will be consider as a distensible, curved artery will be consider, where curved is more reality, and Bifurcation will be consider.

REFERENCES

Agrawal, A.K. and Sengupta S., 1989. "Laminar flow and heat transfer in blocked annuli", J. Numerical Heat Transfer, Part A, Vol.15, PP.489-508.

Aimen, M. A. B., 2005,"Wear monitoring turning processes using vibration and strain measurements", M.Sc.Thesis, University of Baghdad.

Ali, L. Kaeed. 2002,"Numerical study of forced convection over bank of tubes by using body fitted coordinates system "M. Sc .Thesis, University of Technology.

Anderson,D.Jr." Computional Fluid Dynamics: the Basics with Applications" Mc Graw –Hill,Inc.

Anderson, D. A., Pletcher, R.H. and Tannihill, J. C. 1984 "Computational Fluid Mechanics and Heat Transfer",Hemisphere Publishing Corporation.

Bapat , A.2005 " Predicting stenosis in blood vessels " on web. Site

Bramley, J.S., and Sloan, D.M., 1987,"Numerical solution for two –dimensional flow in a branching channel using boundary – fitted coordinates", J. Computers and Fluids, vol. 15, No.3, pp. 297 – 311.

Cebral, J. R., Yim, P. J., Lohner, R., Soto, O., and Choyke, P.L.,2002, " Blood flow modeling in carotid arteries with computational fluid dynamics and MR. Imaging", Academic Rediology , Vol. 9 . No.11, pp. 1286-1299.

Chen, X. May 2003, "A nonlinear viscoelastic Mooney-Rivlin thin wall model for unsteady flow in stenotic arteries", M .Sc .Thesis, Worcester Polytechnic Institute.

Cheng, L.C., Robertson, J.M., and Clark, M.E., 1974,"Calculation of plane pulsatile flow past wall obstacles", J .Computers and Fluids, Vol.2, pp. 363 – 380.

Cox, J.T, Hoften, J. D.A., and Hwang, H.C., 1979,"Investigation of a pulsatile flow field downstream from a model stenosis", J. Biomechanical Engineering, vol. 101, pp. 141–150.

Fletcher, C.A.J., 1987,"ComputationalTechniquesfor Fluid Dynamics 1 ", Springer–Verlag series

Fletcher,C.A.J., 1987,"Computational Techniques for Fluid Dynamics 2 ", Springer – Verlag series.

Guo – Tao liu, Wang, X.J., Ai. B. Q, and Liu, L. G., 2004, "Numerical study of pulsating flow through a tapered artery with stenosis", Chinese J. of Physics, Vol. 42, No. 4 – I.

Hun Jung, Choi, J.W., and Park, C. G., 2004,"Asymmetric flows of non-Newtonian fluids in symmetric stenosed artery", Korea – Australia journal, Vol. 16, No.2, pp. 101-108.

IATRIDIS, M.I., 1987,"A theoretical study of buoyancy driven circulation in a liquid drop ", M.Sc. Thesis, University of Liverpool

Kimmel, E. and Dinnar, V., 1983,"Pulsatile flow in tapered tubes: a model of blood flow with large disturbances", J. Biomechanical Engineering, Vol.105, pp.112–119

Miller, R.W., 1983,"Flow Measurement Engineering Hand Book", Mc Graw – Hill Book Company

Nallasamy, M.1986,"Numerical solution of the separating flow due to an obstruction" J. Computers &Fluids, Vol.14, No. 1, PP.59-68

Ojha, m., Cobbold, C., Johnston, K. W., and Hummel, R.L., 1989."Pulsatile flow through constricted tubes: An experimental investigation using photo chromic tracer methods",J. Fluid Mech., Vol.203 , pp.173-197.

Pontrelli, G., 1999,"Blood flow through an axisymmetric stenosis", Instituto per le applicazioni Del Calcolo–CNR. Viale Del Policlinico,137, 00161 Roma, Italy.

Porenta, G., Young, D.F., and Rogge,T.R., 1985," A finite – element model blood flow in arteries including taper, branches, and obstructions", J. Biomechanical Engineering

Rose, M.L.J., February 1998,"Development of a muscle powered blood pump: fluid mechanic considerations", Ph .D. Thesis University of Glasgow, Department of Cardiac Surgery, Faculty of Medicine.

Taylor, C. A., Hughes, T. J. R., and Zarins, C.K., 1998, "Finite element modeling of three – dimensional pulsatile flow in the abdominal aorta: Relevance to atherosclerosis" Annals of Biomedical Engineering. Vol. 26, pp. 975 – 987.

Varghese, S.S., and Frankel, S. H., 2003,"Numerical modeling of pulsatile turbulent flow in stenotic vessels ',J. of Biomechanical Engineering , Vol. 125 , pp. 445 – 460 .

Walburn, F. J., and Stein, P.D., 1981, "Effect of vessel tapering on the transition to turbulent flow: Implications in the cardiovascular system", J. Biomechanical Engineering, Vol. 103, pp.116 - 120.

Young, D.F., 1979,"Fluid mechanics of arterial stenosis", J. Biomechanical Engineering, Vol.101,pp. 157 – 175.

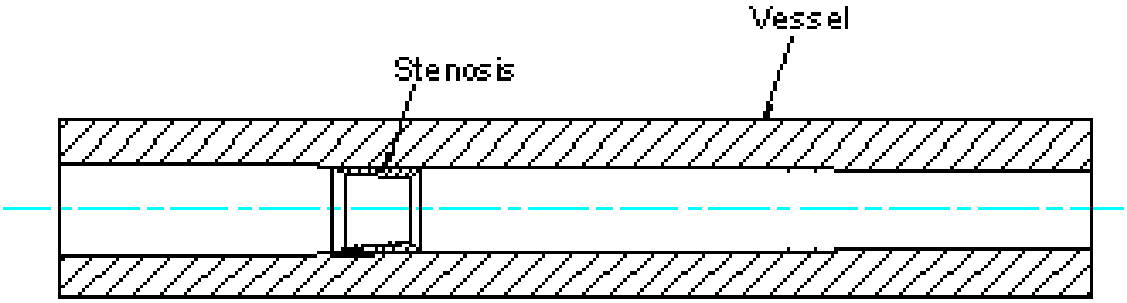

Fig. (1): Schematic of geometry

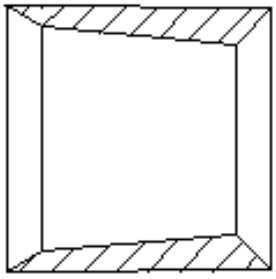

Fig. (2): Geometry of stenosis

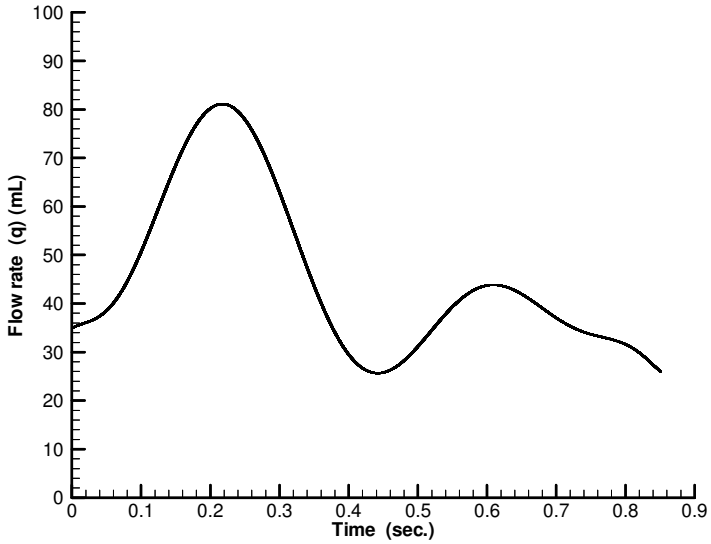

Fig.(3): Physiological flow rate in artery **(Taylor et al 1998)**

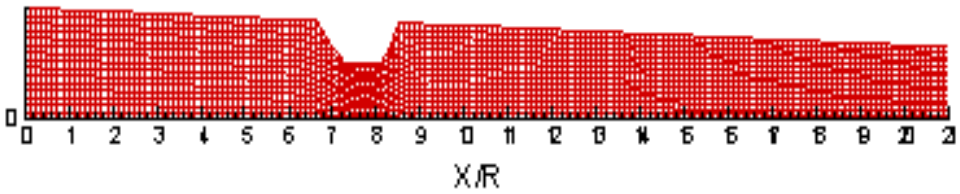

Fig. (4.a): Physical domain

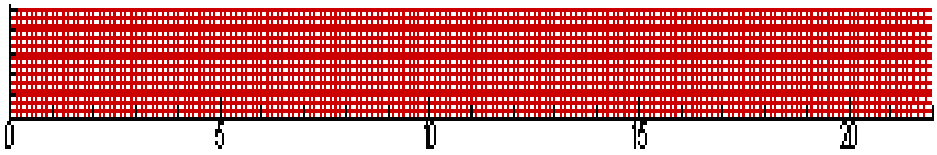

Fig.(4.b): Computational domain.

Fig.(4): Physical and computational domain

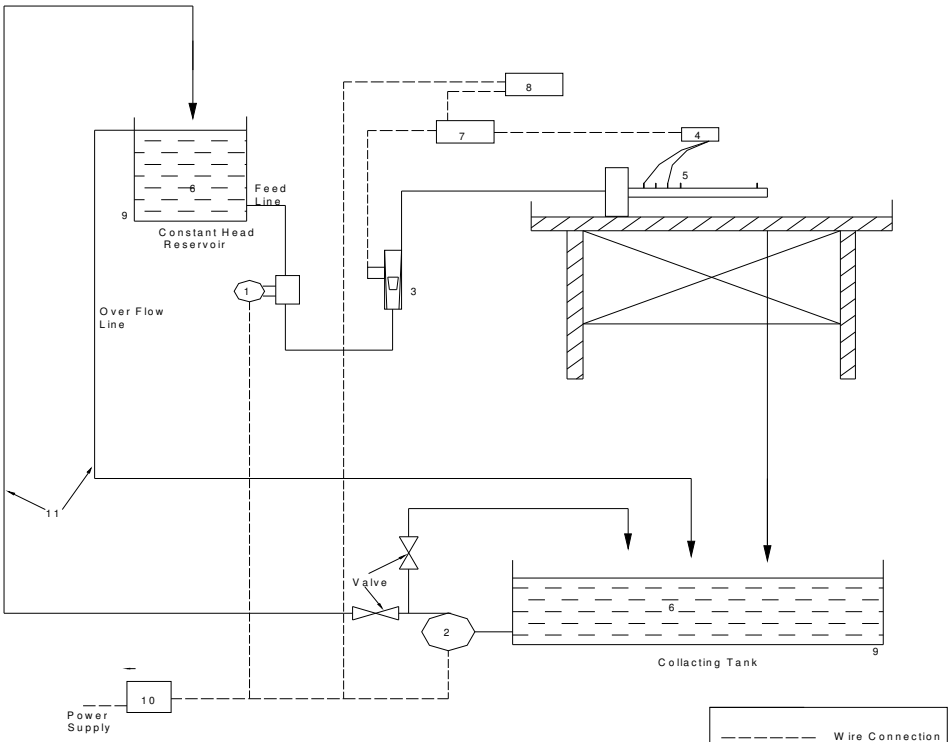

No.	Name of Parts	No.	Name of Parts
1	Dosing Pump	6	Working Fluid
2	Centrifugal Pump	7	Interface Card
3	Flow Meter	8	Computer
4	Pressure Transducer	9	Tank
5	Test Section	10	Stabilizer
11	Hose Connection		

Fig.(5): Experimental rig

Fig.(6): Location of pressure tapes

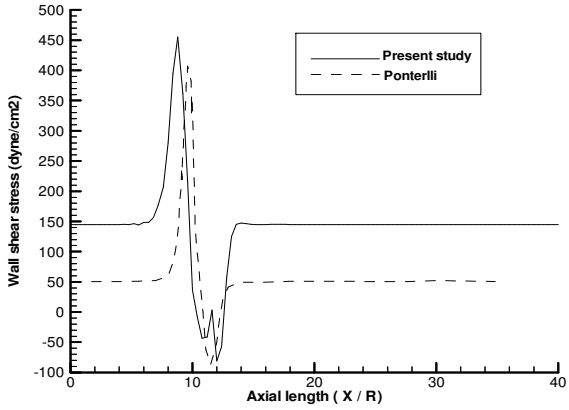

Fig.(7): Comparison of numerical results of wall shear stress (Newtonian fluid) with **(Ponterlli 1999)**.

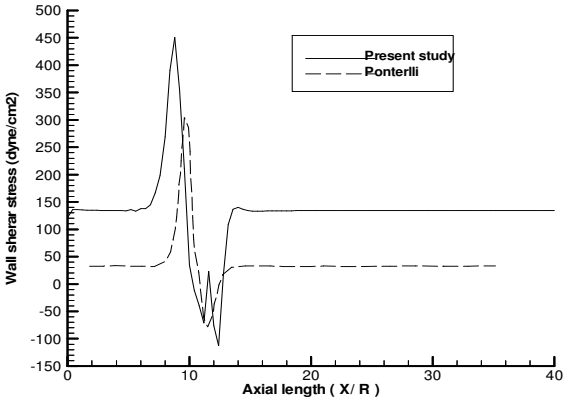

Fig.(8): Comparison of numerical results of wall shear stress (Non Newtonian fluid) with **(Ponterlli 1999)**.

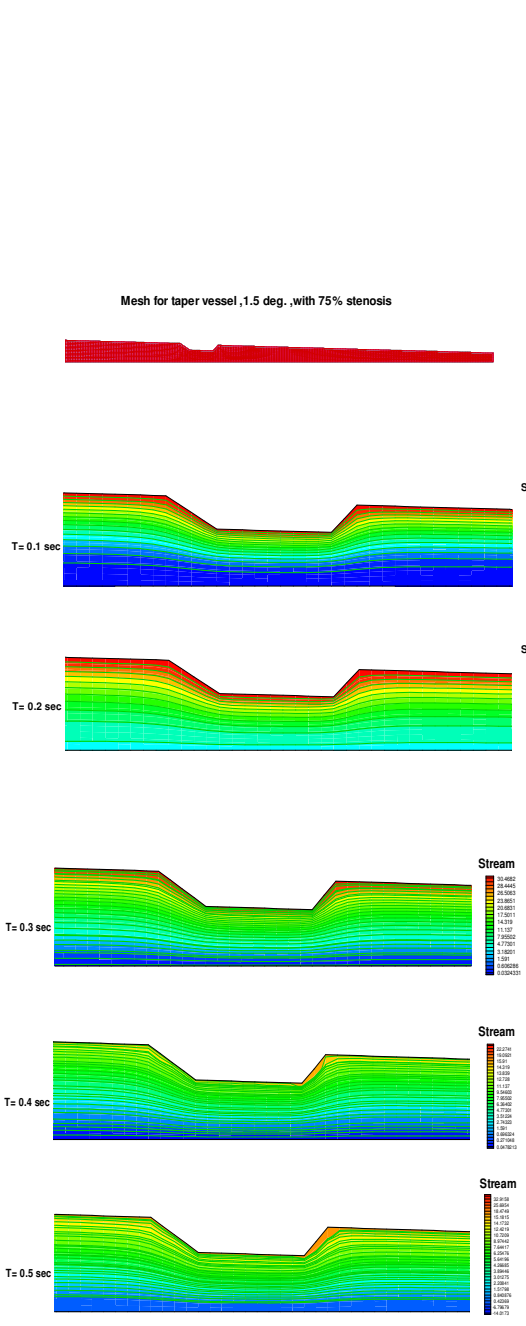

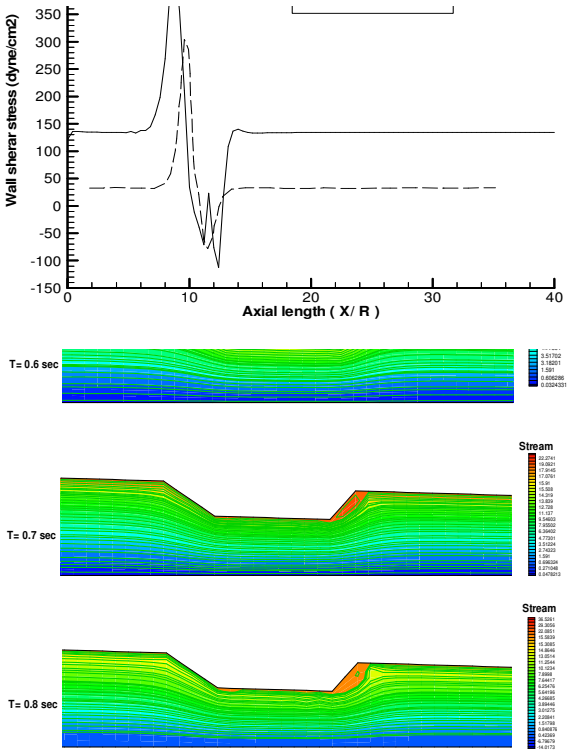

Fig.(9): Instantaneous streamline pattern at different time steps in pulsate flow, for 1.5^{o} taper vessel with 75% stenosis

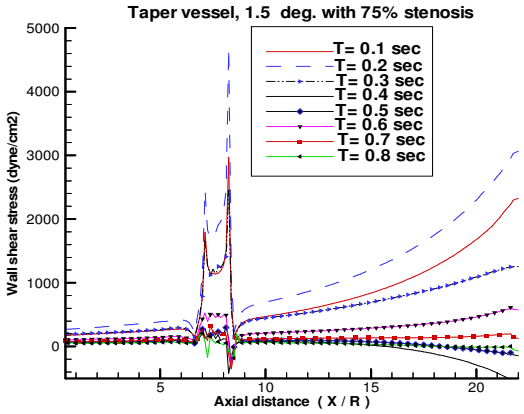

Fig.(10): Wall shear stress at different time steps ,for 1.5° taper vessel with 75% stenosis.

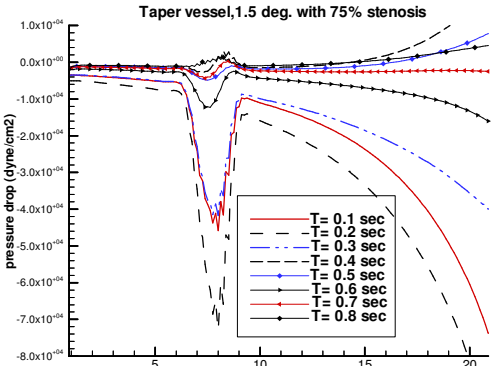

Fig.(11): Pressure drop at different time steps, for 1.5 ° taper vessel with 75% stenosis.

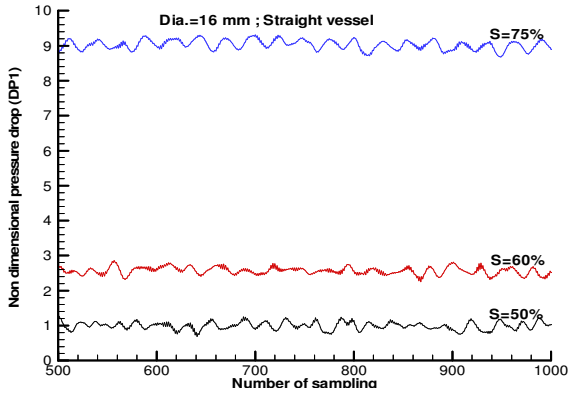

Fig(12): effect of stenosis percent on pressure drop in vessel at flow rate 50ml/s

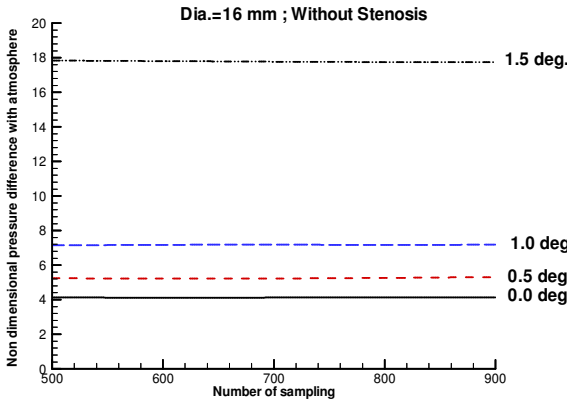

Fig.(13): Effect of tapering angles on pressure in vessel at flow rate 50 ml/sec

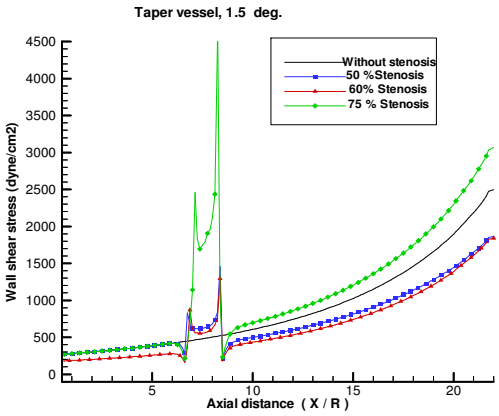

Fig.(14): Effect of stenosis percent on wall shear stress at time step 0.2 sec

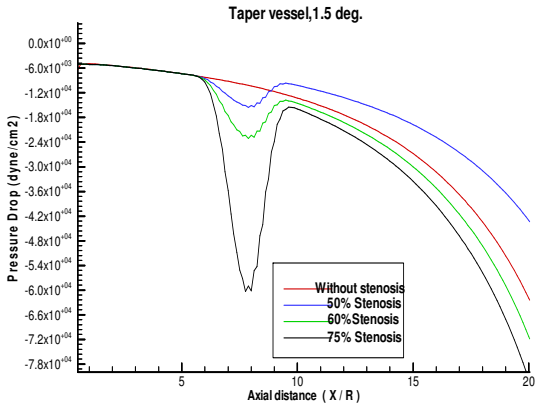

Fig.(15): Effect of stenosis percent on pressure drop at time step 0.2 sec 1.5° taper vessel.

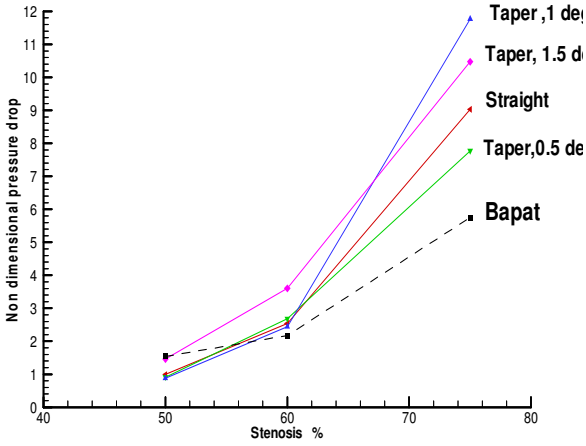

Fig.(16): Comparison of experimental results for different stenosis percent with experimental results of **(Bapat 2005)**.

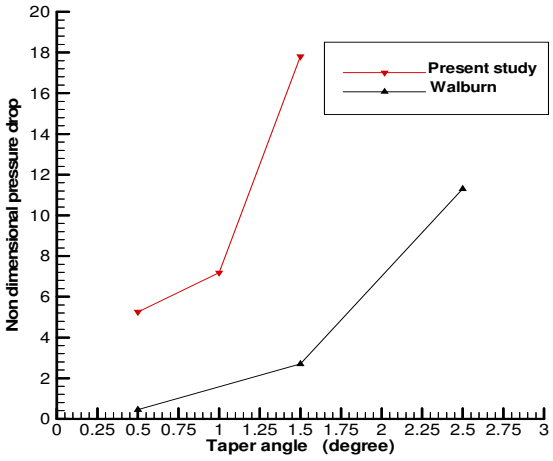

Fig.(17): Comparison of experimental results for tapering angles with experimental results of **(Walburn and Stein 1981)**

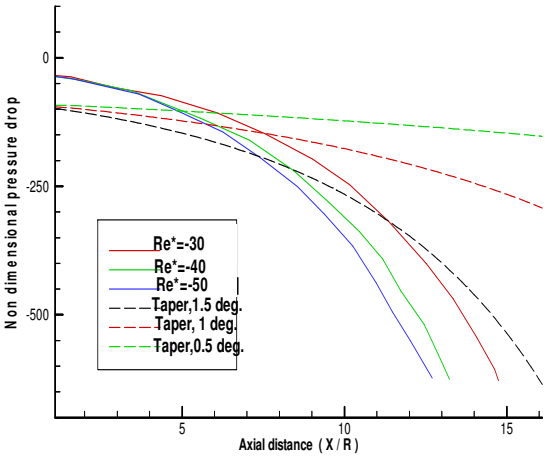

Fig.(18): Comparison of numerical results for tapering angles with numerical results of (**Kimmel and Dinnar 1983)** .

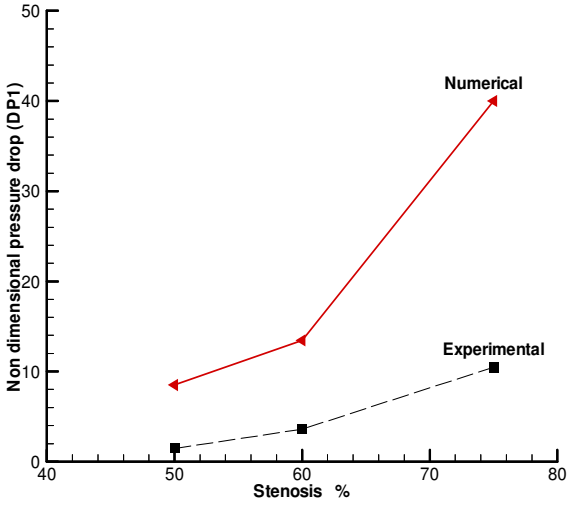

Fig.(19): Comparison of numerical results for different stenosis percent with experimental results for taper vessel 1.5 degree.

NOMENCLATURES

symbol	Meaning	Units
D	Diameter	m
e	Strain rate	1/s
L	length	m
P	Pressure	N/m^2
q	Flow rate	ml/s
r	r-coordinate	
R	Radius	m
Re	Reynolds number $\rho VR/\mu$	
u	Velocity component in x-direction	m/s
v	Velocity component in r-direction	m/s
V	Velocity vector	m/s
x	X-coordinate	
α	Transformation parameter in grid generation	
β	Transformation parameter in grid generation	
γ	Transformation parameter in grid generation	
$\dot{\gamma}$	Shear rate $\dot{\gamma} = \frac{\partial u}{\partial r}$	1/s
δ	$\delta = \frac{\eta_0}{\eta_\infty}$ ratio of asymptotic viscosities at zero to infinity	
ζ	Coordinate in the transformed domain	
η	Coordinate in the transformed domain	
η	Shear viscosity	N/m^2
θ	Taper angle	deg.
λ	Weromsly No.=$R\sqrt{\frac{f}{\nu}}$ ratio of transient inertia force to viscose force	
Λ	Material constant	s
μ	Dynamic viscosity	kg/m.s
ν	Kinematics viscosity	m^2/s
ρ	Fluid density	kg/m^3
τ	Shear stress	N/m^2
ϕ	General dependent function	
$\dot{X}$	Non-dimensional viscosity	
ψ	Stream function	m^2/s
ω	Vorticity	1/s
$\Delta\zeta$	Grid step distance in ζ -direction	
$\Delta\eta$	Grid step distance in η -direction	